Int. J. Solids Structures Vol. 16, pp. 217–229

0020-7683/80/0301-0217/$02.00/0

BUCKLING OF CRACKED MEMBERS UNDER TENSION

KARL MARKSTRÖM and BERTIL STORÅKERS

Department of Strength of Materials and Solid Mechanics, The Royal Institute of Technology, Stockholm, Sweden

(*Received* 23 *May* 1979)

Abstract—The buckling characteristics of cracked elastic plates subjected to uniaxial tensile loads are analysed by aid of a finite element method based upon linear bifurcation theory. The dependence on geometry and boundary conditions of some features of pre-buckling stress states and critical loads and modes are discussed in relation to previous findings for centrally cracked plates. The effect of biaxial loading is considered for one specific geometry. Buckling of three types of edge cracked members is investigated and discussed in particular regarding attainable stress intensity factors at fracture mechanics testing. Statements are made about the interaction of local buckling and fracture. Some phenomena warranting further theoretical consideration are observed.

INTRODUCTION

In a structural member, subjected nominally to tension, zones of compressive stress may develop close to existing cut-outs. As a consequence local buckling may occur. Such an event is undesirable from several viewpoints. Thus, buckling of a local part of a thin-walled structure might severely decrease the natural frequency of the member and possibly end the useful service life and accelerate final fracture. In particular, when the cut-out is a crack, the fracture characteristics are affected. When static loading conditions prevail, the fracture mode may change due to buckling, and in a fatigue process, the rate of crack propagation may be significantly increased as found by Clarkson[1] and others. In the course of fracture mechanics testing of thin cracked specimens, undesired and unavoidable errors, which may totally invalidate the results, may be introduced if buckling is not eliminated.

Local buckling at crack sites has earlier been studied by many workers. Extensive experimental investigations, which have generated many results of practical importance, have been carried out by Dixon and Strannigan[2] and Carlsson *et al.*, see, e.g.[3], and others. As regards theoretical considerations, predominantly Soviet work evidently inspired by Cherepanov's analysis of buckling of membranes[4], has elucidated some matters. The results are of a qualitative rather than quantitative nature as geometry aspects have not been considered in any detail.

For the typical problem of a straight central crack in a plate under nominally uniaxial tension, there exists general agreement that the buckling stress is approximately inversely proportional to the square of the crack length. There seems to be a lack, however, of more systematic theoretical studies of the influence of different geometries and boundary conditions on critical loads. The present investigation is intended as a first step in this direction. Besides centre cracked plates, being analysed in some detail, some edge cracked members, which are important in particular from testing points of view, are dealt with. This issue does not appear to have received any previous attention at all.

SOLUTION METHOD

A typical problem to be solved is illustrated in Fig. 1.

A centrally cracked plate is subjected to a nominally uniaxial stress state. The specific matter to be dealt with is the dependence of the buckling load on the geometric parameters defined in the figure. The plate is assumed to be isotropic and linearly elastic as characterized by Young's modulus E and Poisson's ratio ν.

The approach adopted is based on von Karman's linearized theory for buckling of plates subjected to a pre-buckling state of plane stress. Thus denoting the lateral deflection of the middle surface by $w(x_1,x_2)$ referred to a two-dimensional Cartesian coordinate system x_α, and proceeding from the well-known form of the potential in a buckled state,

$$U = \int \left\{ \frac{Et^2}{12(1-\nu^2)} [w_{,11}^2 + 2\nu w_{,11} w_{,22} + w_{,22}^2 + 2(1-\nu) w_{,12}^2] + (\sigma_{11} w_{,1}{}^2 + 2\sigma_{12} w_{,1} w_{,2} + \sigma_{22} w_{,2}{}^2) \right\} dA \tag{1}$$

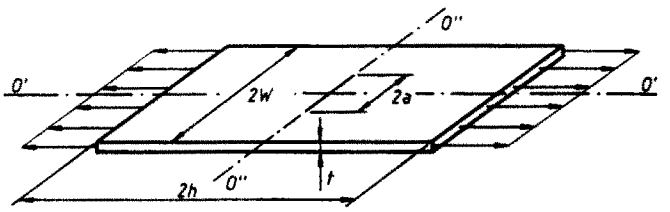

Fig. 1. Dimensions of a plate with a central crack (CC).

adjacent equilibrium states are sought from the variational equation

$$\delta U = 0 \tag{2}$$

a comma denoting partial differentiation with respect to the next subscribed variable and t the plate thickness.

In (1), $\sigma_{\alpha\beta}(x_\gamma)$ denotes the two-dimensional stress field in the pre-buckling state. In all cases treated, this field was computed by aid of a standard finite element program, "NONSAP"[5], assuming Poisson's ratio to be equal to 0.3. To further solve (2) a particular finite element procedure was developed.

As all plates to be considered are of a rectangular shape and the buckling modes were expected to possess certain symmetries, in order to evaluate U in (1), one half or alternatively one quarter of each member were discretized into a set of 64 rectangular plane elements of dimensions $2b \times 2c \times t$ with slight variations in some cases. The local displacement field was approximated by

$$\begin{aligned} w/t = {} & c_1 + c_2 x/b + c_3 y/c + c_4 xy/(bc) + c_5(1 - x^2/b^2) \\ & + c_6(1 - y^2/c^2) + c_7(1 - x^2/b^2)x/b + c_8(1 - y^2/c^2)y/c \end{aligned} \tag{3}$$

referred to a local coordinate system xy†.

In order to ascertain continuity of corner displacements and slopes at the mid-point of interelement boundaries, these variables were selected as generalized coordinates, m_i, for an element, rendering the element eight degrees of freedom.

Stated in this form, the adopted element, originally proposed by Bäcklund[6] and later modified by Pettersson[7], has earlier been successfully employed in analyses of plate bending. Evidently the mode function given in (3) is bi-harmonic.

After referring the local constants, $c_1 \ldots . c_8$, in (3) to the one-dimensional generalized coordinate matrix $\mathbf{m}$, it is a routine procedure, although a tedious one, to explicitly evaluate the functional U on the form

$$U = \mathbf{m}^T(\mathbf{A} + \mathbf{S})\mathbf{m} \tag{4}$$

in terms of a global coordinate system, where $\mathbf{A}$ is the assembled stiffness matrix and $\mathbf{S}$ the corresponding stress matrix. In the computation of the pre-buckling state, $\mathbf{S}$, constant stress elements were employed.

Equation (2) now reduces to the homogeneous relation

$$(\mathbf{A} + \mathbf{S})\mathbf{m} = \mathbf{0} \tag{5}$$

where $\mathbf{m}$ is the assembled (global) eigen-vector.

By definition the symmetric matrix $\mathbf{A} + \mathbf{S}$ becomes positive semi-definite when the first eigen-state is reached. In order to determine this event, the matrix in question was subjected to Cholewski decomposition and the eigen-load was determined as the one making one diagonal element in the decomposed matrix vanish. This procedure did guarantee that the first eigen-

†The writers are indebted to Dr. J. Bäcklund, The University of Linköping, Sweden for proposing this element.

state was always detected. Once the eigen-value had been determined, the associated eigen-vector was computed by standard methods.

The described finite element model was tested for accuracy and convergence in two cases for which exact solutions are known; uniform uni-directional compression of a quadratic plate and uniform pure shearing of a rectangular plate simply supported at all edges. In both cases the buckling stress may be expressed as

$$\sigma_{cr} = k\frac{\pi^2 E}{1-\nu^2}\left(\frac{t}{L}\right)^2 \tag{6}$$

where k is a geometry and load dependent factor while L is the shortest width of the plate.

The width ratio of the sheared plate was chosen as 1.25 in order to render possible a comparison with some classical finite element results given by Kapur and Hartz[8]. The exact values of the factor k in eqn (6) is then given by 4.00 for compression and 7.71 for shearing.

The percentage errors for the buckling load obtained for different grid sizes by the present method and that of Kapur and Hartz are given in the table below.

		Percentage errors						
Grid size		2×2	3×3	4×4	6×6	8×8	10×10	12×12
Uniform uniaxial compression	Ref. [8]		−8.88	−5.75	−2.80	−1.65	−1.00	−0.58
	Present method	−13.0	−7.1	−4.1	−1.9	−1.0		
Uniform shearing	Ref. [8]			−9.92	−6.00	−3.37		
	Present method			−5.4	−2.5	−1.2		

Judging from this table, the accuracy and convergence may be considered acceptable, in particular when remembering that the present element has got eight degrees of freedom in contrast to twelve in[8].

A comparison of the efficiency of several modern hybrid element models has been recently carried out by Brandt[9], for the two loading cases dealt with above. It turns out that the present element compares favourably in particular for coarse grids.

RESULTS AND DISCUSSION

With reference to Figs. 1 and 2, plates of dimensions given in the table below were analysed.

Geometry	a/W	h/W
CC	1/4, 3/8, 1/2, 5/8, 3/4	1/2, 1, 2
CT	9/20, 1/2, 11/20	
SEN	7/10, 3/4, 4/5	
DEC	7/10, 3/4, 4/5	

The length of central cracks subjected to investigation were bounded from above and below by the requirement that any characteristic length should not fall below two element length units. Similarly for edge cracked members, the uncracked ligament spanned at least four mesh intervals.

In all members subjected to edge loads, as regards out of plane deflection, the loaded part of the boundary was assumed clamped and the remainder free. The geometry denoted by CT in Fig. 2 was chosen in order to model a compact tension test specimen.

For the two geometries (CC and DEC) possessing double symmetry, buckling modes being symmetric with respect to the axis O′O′ were investigated. As regards the symmetry axis O″O″, being common to all members, both symmetric and antisymmetric modes were sought for.

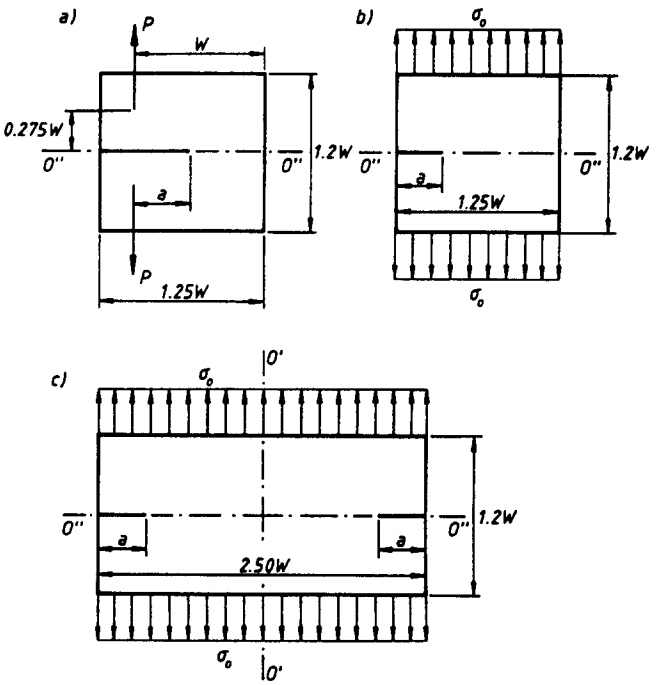

Fig. 2. Dimensions of edge cracked plates, (a) CT, (b) SEN, (c) DEC.

(i) *Centre cracked plates*

In their investigation of centre cracked plates, Dixon and Strannigan[2] carried out some interesting measurements concerning the inhomogeneous pre-buckling stress state by aid of photoelasticity. In particular these workers determined the magnitude of the largest compressive stress component in plates of various geometries. This stress acts at the centre of the crack faces in a direction transverse to that of the external loading.

In Fig. 3 experimental and presently obtained theoretical results are compared as regards this matter. The close agreement gives some confidence in the numerical method employed to

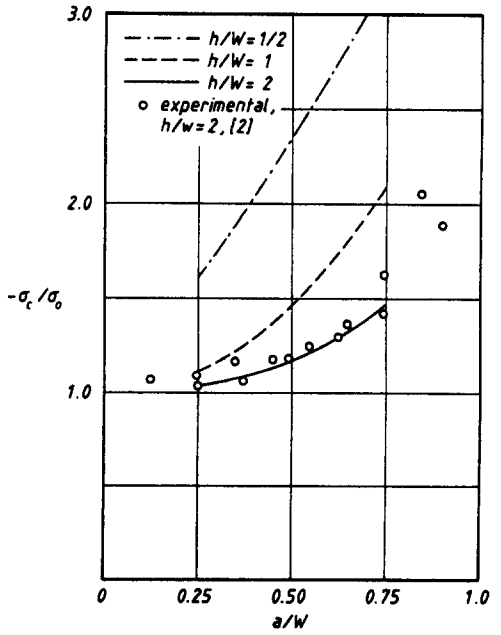

Fig. 3. Maximum compressive stress as function of crack length.

determine the pre-buckling state. It is obvious from Fig. 3 that, for a plate of given width, the largest compressive stress varies significantly with the crack length to plate length ratio.

For a plate of finite width, the region of high compressive stress is larger than for one of infinite width. As for a given geometry, the magnitude of the compressive stress diminishes along the O'O'-direction (Fig. 1), the difference between the principal stresses attains a relative minimum. The location of this minimum value was also determined by Dixon and Strannigan. The relative distance of this point from the crack with respect to crack length was found by these investigators to increase slightly with crack length from the theoretical value of $1/\sqrt{2}$ at vanishing crack length. In the present analysis this quantity was almost independent of crack length and if any tendency at all was to be traced, it was one of decrease.

In order to investigate the role of boundary conditions regarding the pre-buckling stress state, for one geometry ($a/W = 1/2$, $h/W = 1$) uniform longitudinal boundary displacements were enforced in contrast to axial traction. The shapes of zones suffering under compressive stresses are indicated in Fig. 4 for the two cases. As a typical value in the former case, the magnitude of compressive stress components were around 30% less at the same nominal load. Judging from the findings of Dixon and Strannigan, it would seem then that their testing conditions would correspond closely to prescribed traction.

The relevant buckling results for the centre cracked plates are reproduced in Figs. 5–10. For all geometries investigated, the lowest buckling load was associated with the symmetric mode depicted in Fig. 7. Based on their experimental findings, Dixon and Strannigan observed, without stating further details, this mode to be the most common.

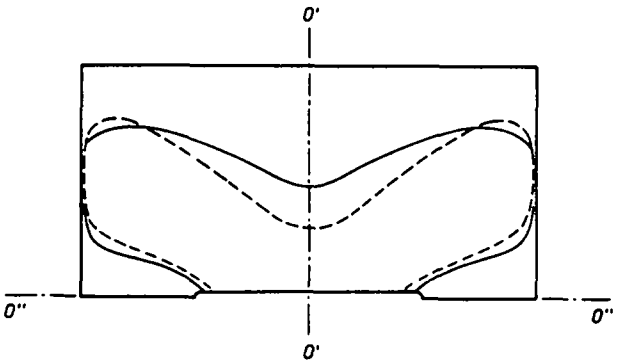

Fig. 4. Zones under compression; —— boundary conditions of traction, ---- of place.

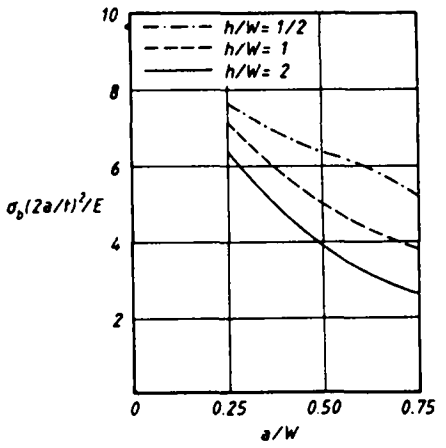

Fig. 5.

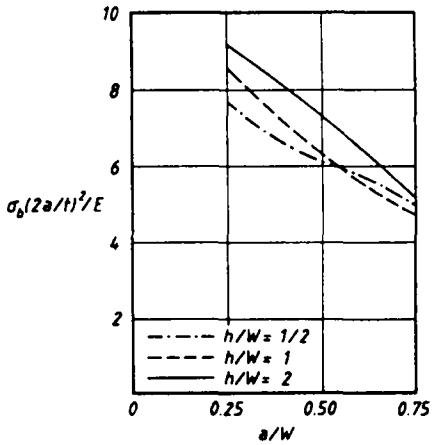

Fig. 6.

Fig. 5. Buckling loads for centre cracked plates (CC), symmetric mode.

Fig. 6. Buckling loads for centre cracked plates (CC), antisymmetric mode.

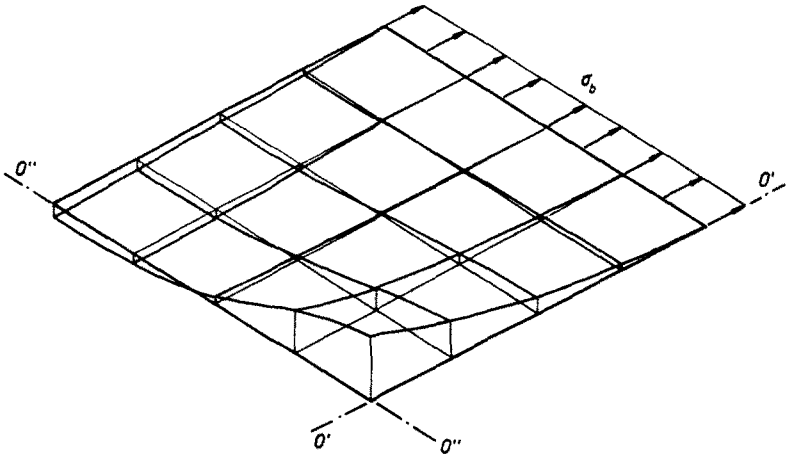

Fig. 7. Symmetric buckling mode for a centre cracked plate ($a/W = 1/2$).

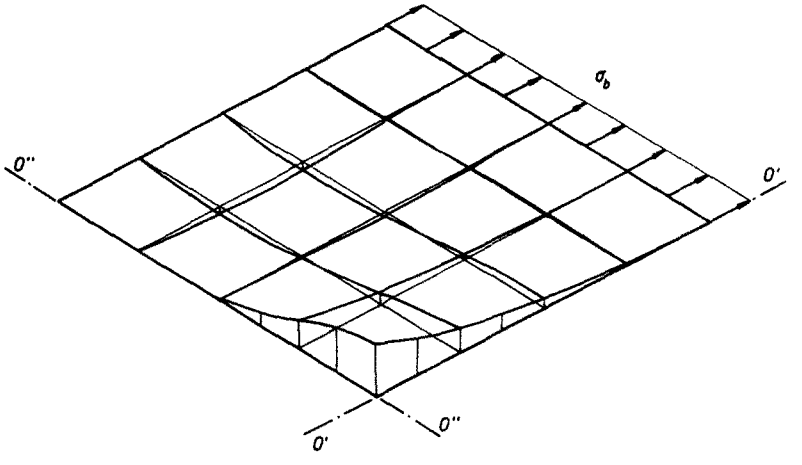

Fig. 8. Antisymmetric buckling mode for a centre cracked plate ($a/W = 1/2$).

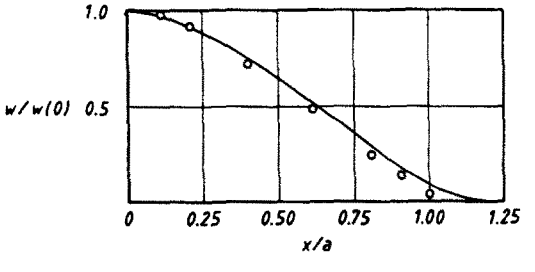

Fig. 9.

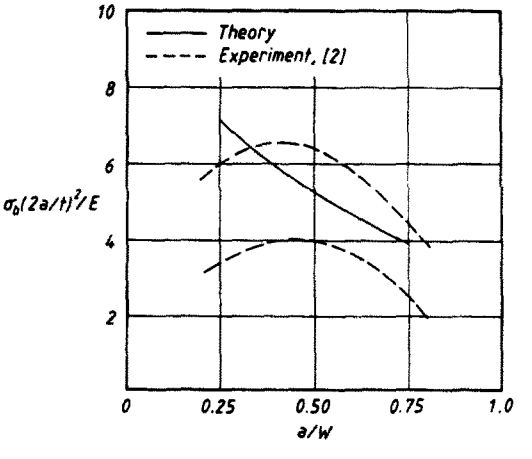

Fig. 10.

Fig. 9. Buckled shape along crack face, — theory, O experiment[10].

Fig. 10. Theoretical and experimental (lower and upper bounds) buckling loads for centre cracked plates, symmetric mode ($h/W = 1$).

The buckled shape at the crack face is shown in more detail in Fig. 9, where it is compared with findings in a solid investigation by Petyt[10] mainly devoted to vibration characteristics of cracked plates. It should be noted though that, in Petyt's experiments, the investigated plate was geometrically characterized by $a/W = 0.35$, $h/W = 1.35$ while the present calculations are based on $a/W = 0.50$, $h/W = 1.00$.

From Fig. 5 it may be concluded that the critical load for symmetric buckling decreases with the length of the plate while for the antisymmetric case the contrary is essentially true as may be seen in Fig. 6. For the shortest plate, however, the buckling curve exhibits a somewhat unexpected change of rate of curvature at larger crack lengths. This may be due to some numerical instability caused by adjacent eigen-values. To further examine this, two cases of different crack length ($a/W = 5/8$ and $3/4$) were re-computed with a refined mesh (twice as many elements). The effect still persisted but the theoretical buckling load was lowered by 7%. The curve depicted in Fig. 6 is in fact a result of the refined analysis.

In Fig. 10 theoretical critical loads are compared with experimental results of Dixon and Strannigan. The outcome is encouraging except at shorter crack lengths.

In essence the present results are obtained by aid of a linear bifurcation analysis based on the assumption of a perfect pre-buckling plate shape. In their investigation of the behaviour of real (imperfect) cracked plates, Dixon and Strannigan have defined upper and lower bounds for the actual buckling load. Their strategy in doing so is illustrated in Fig. 11.

The lower limit was defined as the stage when the bending strain of the plate, in the vicinity of the crack, commenced to increase rapidly with the external load. The upper limit was taken as the external load value when the bending rate had again reached an approximately constant value.

Although at the shortest crack length ($a/W = 1/4$) presently dealt with, the crack comprises only four element length units with deteriorating numerical accuracy as a possible consequence, it still remains in doubt whether the trend of decreasing non-dimensional buckling values at shorter crack lengths has got any theoretical support from the bifurcation point of view. It must be rembered that the discrepancy under discussion may be intimately connected with the presence of initial imperfections and the ambiguity in defining buckling of real systems subjected to testing, which make any firm conclusions hard to draw. This is further evidenced in a vast gathering of experimental results regarding thin slotted sheets by Zielsdorff and Carlson[3].

These writers have proposed an empirical formula applicable to buckling of plates perforated by slits or holes and subjected to uni-directional loading. For the degenerate case of a centre cracked plate under uniaxial tension, Carlson and Zielsdorff's formula for the buckling load reduces to

$$\sigma_b/E = k(t/2a)^2 \tag{7}$$

in the present notation, the constant k being equal to 4.18.

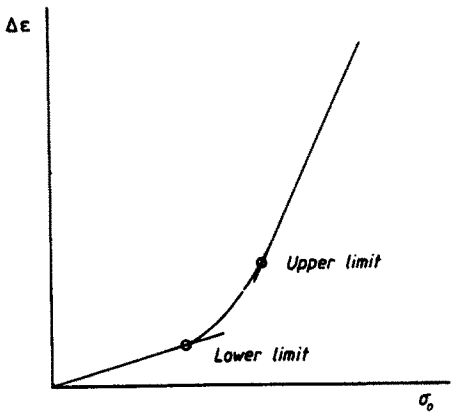

Fig. 11. Bending strain at crack as function of external load.

In their investigation of cracked plates having dimensions $1/6 \leq a/W \leq 1/3$, $h/W = 5/3$, Carlson and Zielsdorff determined buckling loads, essentially by aid of a modified Southwell plot, which were well reproduced by the above formula (7). Compared with the results of the present bifurcation theory, this formula underestimates the buckling load for shorter crack lengths by a factor of the order of two. Apart from the fact that the factor k must necessarily depend on Poisson's ratio, it is apparent also from the tests of Carlson and Zielsdorff that experimentally determined results do not lend themselves to a unique definition of buckling and are indeed sensitive to initial imperfections. Another empirical formula based on vibration experiments and yielding $k = 4.72$ in (7), has been proposed by Clarkson[1].

Results from vibration experiments carried out by Petyt[10] may be interpreted as though a buckling curve corresponding to that of Fig. 10, should have a maximum at $a/W = 1/6$ approximately.

Another aspect, which is relevant to this issue, is the role of the boundary conditions. In order to investigate the significance of the manner the external loading is applied, buckling of a centre cracked plate with enforced uniform longitudinal in-plane boundary displacements in contrast to traction, was analysed. It was found then that for a plate characterized by $a/W = 1/2$, $h/W = 1$, the nominal load at both symmetric and antisymmetric buckling was increased by approximately 50%. This finding adds further difficulties to the comparison between theoretical and experimental results.

In order to settle the matter regarding buckling loads at small crack length to width ratios, existing theoretical studies do not offer much help. Calculations for a crack of finite length in a seemingly infinite plate have been carried out by Litvinenkova[11] resulting in a value of 3.5 for the factor k in (7). Substantially, however, the analysis was based on an essentially uniaxial pre-buckling stress state in a strip of finite width ($a/W = 1/2$) and carried out rather crudely by aid of a Rayleigh–Ritz procedure. It must be concluded that the result obtained bears no conviction as regards the issue under discussion. In addition, from application of an approximate variational procedure, somewhat difficult to grasp, Guz *et al.*[12,13] have reported a k-value of 4.04.

At this instant it should be clear that the presence of a transverse external load component will substantially affect the tendency of a plate to buckle. Finally then for the case of a central crack, the effect on the buckling stress, $\sigma_b^* = \sigma_b/\sigma_b(\sigma_t = 0)$, of a transverse stress, σ_t, was investigated. The particular geometric characteristics singled out for study were $a/W = 1/2$, $h/W = 1$. The results are shown in Fig. 12.

The effect is very pronounced and in particular it may be seen that at the stress ratio of one half, the axial buckling stress is increased by a factor of four. This result should be of immediate interest as regards crack behaviour in thin-walled pressure vessels and air fuselages.

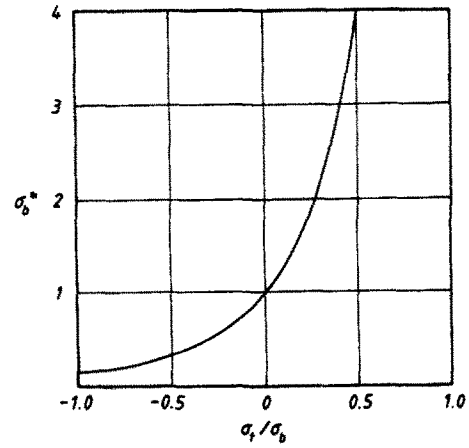

Fig. 12. Normalized buckling loads for a centre cracked plate as function of transverse stress, symmetric mode ($a/W = 1/2$, $h/W = 1$).

(ii) *Compact tension test specimens*

Mainly to achieve results useful at fracture mechanics testing, the CT-geometry depicted in Fig. 2 was analysed similarly as above. The relative crack length (a/W) was varied between 0.45 and 0.55 in accordance with ASTM specifications. For all edge cracked members depicted in Fig. 2, CT, SEN and DEC, the width to thickness ratio was chosen as 250 (the stress state at initiation of buckling in case of arbitrary thickness being determinable from its dependence on squared plate thickness according to (1)).

The main results for the CT-specimen are given in Figs. 13–15. In order to possibly obtain lower bounds as regards buckling at realistic testing conditions, out of plane constraints were introduced only as to suppress rigid body motion. Besides constraints due to anticipated symmetry or antisymmetry, for the symmetric mode only rotation was suppressed around an in-plane axis in the load direction at the points of attack of the loading forces.

It should be underlined that the non-dimensional buckling loads indicated in Fig. 13 are to be regarded as estimates. The uncracked part of the ligament $O''O''$, shown in Figs. 14 and 15, was comprised at the longest crack by only four element length units. In fact a change from three to four elements increased the critical load by almost 50%.

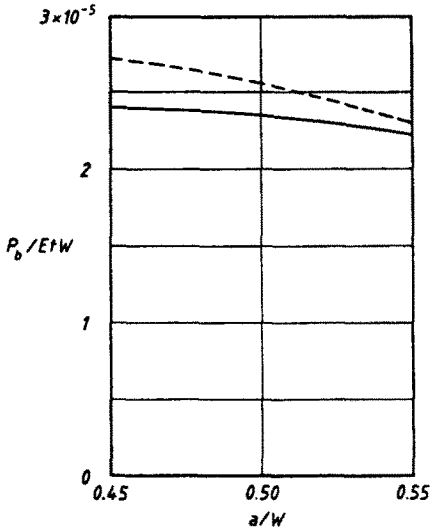

Fig. 13. Buckling loads for compact tension test specimens (CT), (——) symmetric and (----) antisymmetric modes.

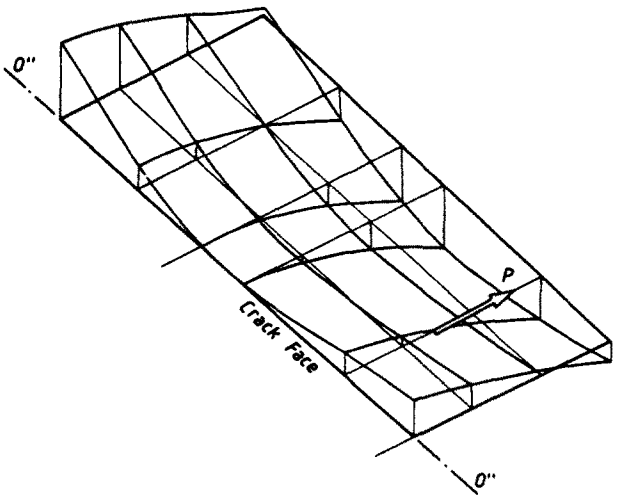

Fig. 14. Symmetric buckling mode for a compact tension test specimen ($a/W = 1/2$).

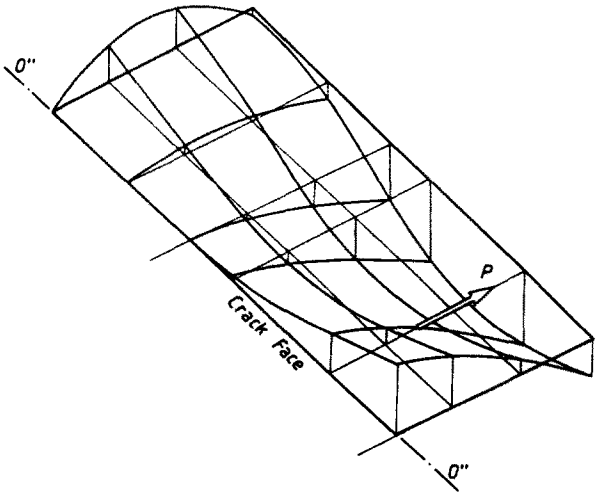

Fig. 15. Antisymmetric buckling mode for a compact tension test specimen ($a/W = 1/2$).

To the best of our knowledge no theoretical or experimental results for CT-specimens are available for comparison. Drawing upon the first writer's experience of routine fracture mechanics testing, however, the achieved results are realistic.

Although, as may be seen in Fig. 13, the external load at buckling decreases with crack length, it is readily shown by aid of any standard hand-book, that the reverse is true for the stress intensity factor at buckling.

(iii) *Edge notched plates*

Calculations for single edge notched members (SEN) were carried out with identical geometric parameters as for the CT-specimen. The different definitions of crack length, shown in Fig. 2, should be noted though. As no additional results are available for comparison, the outcome, depicted in Figs. 16–18, is left without detailed comments.

It is evident from Fig. 16 that under loading of uniform traction, the first critical mode is anti-symmetric. In this case, however, the dependence of the buckling load on crack length is more pronounced and the magnitude of the stress intensity factor at critical load decreases with crack length. At the event of buckling, this factor is approximately four times higher for the shortest crack dealt with and two times higher for the longest crack as compared to the CT-specimen.

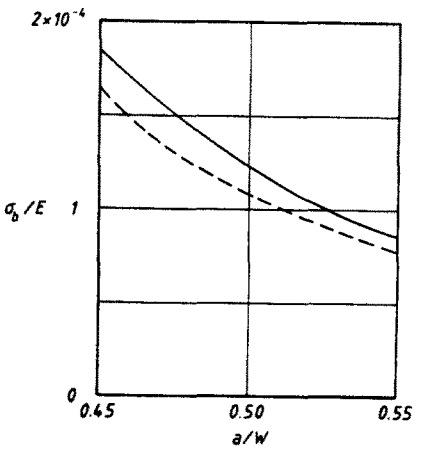

Fig. 16. Buckling loads for single edge notched plates (SEN), (——) symmetric and (- - - -) antisymmetric modes.

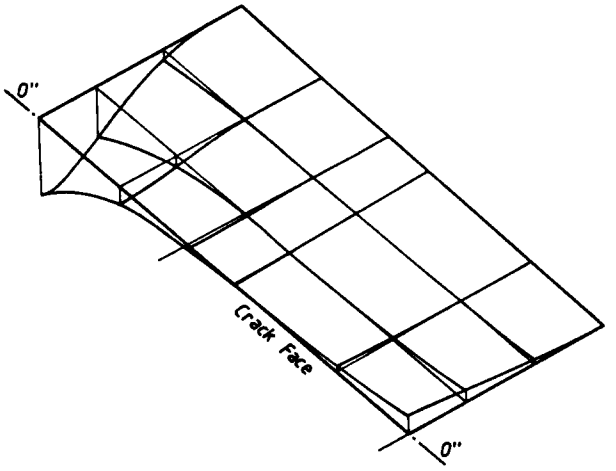

Fig. 17. Symmetric buckling mode for a single edge notched plate ($a/W = 3/4$).

Finally for the geometry with two symmetric edge cracks (DEC) a comparison of the essential features of the pre-buckling stress state was made with results based on an electrical analogue and reported by Redshaw and Rushton[14]. The different geometries involved did not permit a close quantitative comparison but the shapes of the compressed zone and the stress trajectories were on the whole very similar.

The buckling results are given in Figs. 19–21. Incidentally for this geometry and loading conditions, the present numerical method did not separate the eigen-values of symmetric and antisymmetric modes. From the view-point of efficiency as a test specimen and judging from stress intensity factors for a somewhat longer specimen ($h/W = 1$), the attainable pre-buckling stress intensity factor decreases with crack length but is roughly 50% higher than for a single edge notched specimen having the same crack length and thickness.

Contemplating the shape of the symmetric mode in Fig. 20, it is conceivable that the type of constraints prevailing at the loaded edge is important as regards the magnitude of the buckling load. Still more it should be remembered that for this case and that of central cracks, all conclusions drawn are based upon the assumption of buckling modes being symmetric with respect to an axis (O'O') parallel to the load direction.

CLOSURE

It is believed that the results presented above might be useful both for structural design and various fracture considerations. It is tempting, in particular for the case of central cracks, to summarize the results as regards the role of geometry parameters by aid of a single formula. As

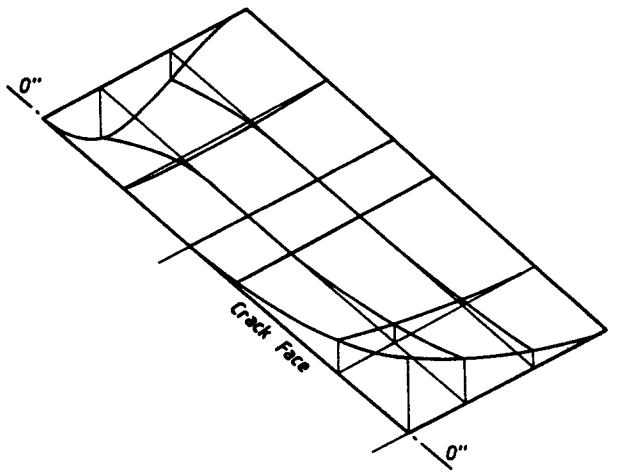

Fig. 18. Antisymmetric buckling mode for a single edge notched plate ($a/W = 3/4$).

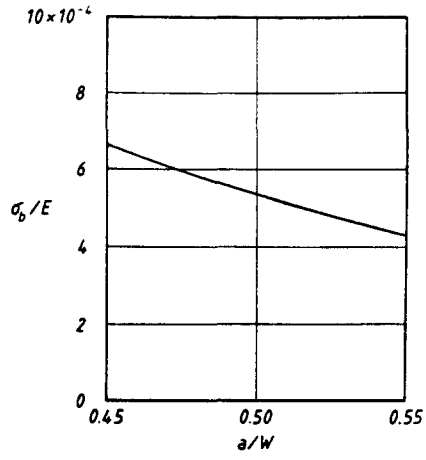

Fig. 19. Buckling loads for double edge cracked plates (DEC).

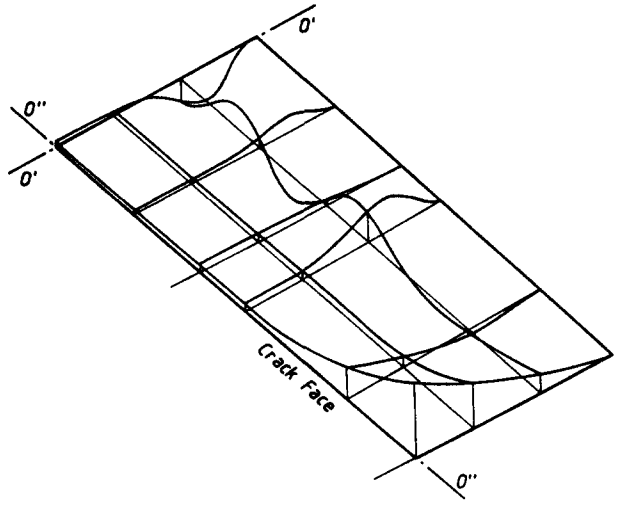

Fig. 20. Symmetric buckling mode for a double edge cracked plate ($a/W = 3/4$).

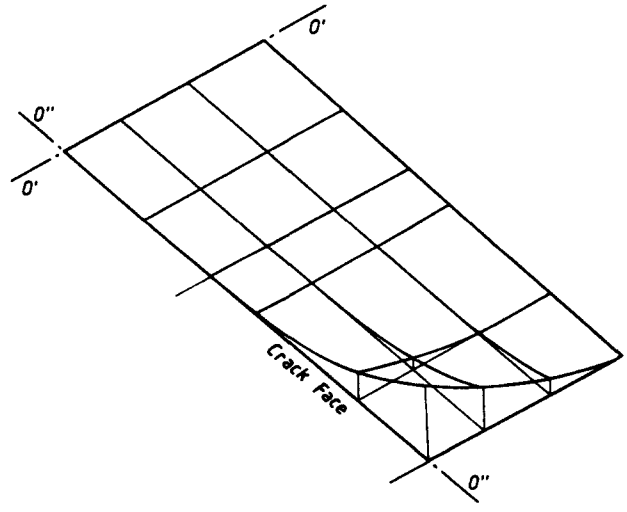

Fig. 21. Antisymmetric buckling mode for a double edge cracked plate ($a/W = 3/4$).

the present numerical method did become inaccurate at short cracks, however, this is abstained from until further details are known of this state of affairs. To investigate this matter, more sophisticated computer facilities, than were presently available, are needed.

For Griffith type fracture the critical stress is approximately proportional to the inverse square root of the crack length while at buckling the same is true for the inverse square of crack length. Thus from the present results, critical crack lengths may be determined, at which a change between these two pure failure modes may be predicted to occur. The utilized mathematical model is, however, very simple. In real metals for instance, plastic zones will start to grow at crack tips, which might severely influence the local stress field. Thus plastic zone growth and the event of buckling interacts in an involved manner in which the thickness of the plate plays a central role as was emphasized by Dixon and Strannigan. Thus for thicker plates this effect may not be disregarded.

Based on theoretical and experimental evidence, the systems under discussion are not imperfection-sensitive in ordinary sense. The existence of small initial geometric imperfections, which grow with the amount of external loading, might, however, drastically change the fracture behaviour of cracked members. Thus, apart from a possible change of fracture mode, local buckling will increase the stress concentration factor at cracks (of finite tip radius). It was found by Dixon and Strannigan for instance that, in case of a crack tip radius to crack length ratio of 1.25%, the maximum stress increased by 20% at an out-of-plane deflection of 5% of the crack length. The static strength of cracked aluminum plates free to buckle was on the average about 10% lower than when buckling was restrained. This perhaps unexpectedly low reduction of strength was thought to be due to the occurrence of considerable plastic flow at crack tips. Higher reductions (of the order of 40%) have been found for steel. Similar effects are also active in fatigue processes.

The deformation behaviour of an imperfect cracked plate has in fact been analysed earlier by Petyt for one particular case. By introducing a geometric imperfection of the same shape as the bifurcation buckling mode, this writer found a deformation course at the crack, which was qualitatively the same as depicted in Fig. 11 above. The deflection pattern did not change appreciabely during progressing deformation. A general post-buckling analysis is still lacking though.

Furthermore, whatever will be the final failure mechanism of a shallow cracked member, both in-plane and out-of-plane boundary constraints will play a central role. This aspect and the additional points raised seem worthy of additional theoretical consideration. This is, however, left for further study.

REFERENCES

1. B. L. Clarkson, The propagation of fatigue cracks in a tensioned plate subjected to acoustic load. In *Acoustical fatigue in aerospace structures* (Edited by W. J. Trapp and D. Forney), p. 361. Syracuse University Press, Syracuse, New York (1965).
2. R. Dixon and J. S. Strannigan, Stress distribution and buckling in thin sheets with central slits. *Proc. 2nd Int. Conf. on Fract.*, Brighton, 105 (1969).
3. G. F. Zielsdorff and R. L. Carlson, On the buckling of thin tensioned sheets with cracks and slots. *Engng Fract. Mech.* 4, 939 (1972).
4. G. P. Cherepanov, On the buckling under tension of a membrane containing holes. *PMM* 27, 275 (1963); *J. Appl. Maths Mech.* 27, 405 (1963).
5. K. J. Bathe, E. L. Wilson and R. H. Iding, NONSAP, a structural analysis program for static and dynamic response of nonlinear systems. *Struct. Engng Lab.*, Univ. of California, Rep. UC SESM, 74-3 (1974).
6. J. Bäcklund, *Mixed finite element analysis of plates in bending. Small deflection theory of elastic and elasto-plastic plates.* Department of Structural Mechanics, Chalmers University of Technology, Publication 71:4, Gothenburg (1971).
7. H. Pettersson, *A mixed finite element for the calculation of rectangular plates.* Department of Building Construction, Chalmers University of Technology, Publication 72:1, Gothenburg (1972) (in Swedish).
8. K. K. Kapur and B. J. Hartz, Stability of plates using the finite element method. *J. Engng Mech. Div., Proc. ASCE* 92, 177 (1966).
9. K. Brandt, Derivation of geometric stiffness matrix for finite element hybrid models. *Int. J. Solids Structures* 14, 53 (1978).
10. M. Petyt, The vibration characteristics of a tensioned plate containing a crack. *J. Sound Vib.* 8, 377 (1968).
11. Z. N. Litvinenkova, On the stability of a stretched plate with an inner crack. *IZV. ANUSSR Mekh. tver. tela* 5, 148 (1973).
12. A. N. Guz, G. G. Kuliev and I. A. Tsurpal, A contribution to the theory of fracture of solid bodies. *Prikl. mekh.* 11, 32 (1975).
13. A. N. Guz, G. G. Kuliev and I. A. Tsurpal, On fracture of brittle materials from loss of stability near a crack. *Engng Fract. Mech.* 10, 401 (1978).
14. S. C. Redshaw and K. R. Rushton, An electrical analogue solution for the stresses near a crack or hole in a flat plate. *J. Mech. Phys. Solids* 8, 173 (1960).